Journal of Non-Crystalline Solids 552 (2021) 120454

Contents lists available at ScienceDirect

Journal of Non-Crystalline Solids

journal homepage: www.elsevier.com/locate/jnoncrysol

The detailed calculations of optical properties of indium-doped CdO nanostructured films using Kramers-Kronig relations

V. Ganesh[a], L. Haritha[b], H. Elhosiny Ali[a,c], A.M. Aboraia[d,e], Yasmin Khairy[c], H.H. Hegazy[a,e], V. Butova[d], Alexander V. Soldatov[d], H. Algarni[a], H.Y. Zahran[a,f], I.S. Yahia[a,f,g,*]

[a] Advanced Functional Materials & Optoelectronic Laboratory (AFMOL), Department of Physics, Faculty of Science, King Khalid University, P.O. Box 9004, Abha, Saudi Arabia
[b] Department of Physics, Telangana University, P.O. Box 503101, Nizamabad, Telangana state, India
[c] Physics Department, Faculty of Science, Zagazig University, Zagazig, 44519, Egypt
[d] The Smart Materials Research Institute, Southern Federal University, Sladkova 178/24, 344090, Rostov-on-Don, Russia
[e] Department of Physics, Faculty of Science, Al-Azhar University, Assiut, 71542, Egypt
[f] Nanoscience Laboratory for Environmental and Bio-medical Applications (NLEBA), Semiconductor Lab., Metallurgical Lab.1, Physics Department, Faculty of Education, Ain Shams University, Roxy, 11757, Cairo, Egypt
[g] Research Center for Advanced Materials Science (RCAMS), King Khalid University, P.O. Box 9004, Abha 61413, Saudi Arabia

ARTICLE INFO

Keywords:
Indium-doped CdO
Nanostructured films
Spin coating technique
Linear/nonlinear optical parameters
Kramers-Kroning relations

ABSTRACT

The different ratios of Indium-doped cadmium oxide thin films were deposited on a glass substrate by a sol-gel assisted spin coating technique. The structure of the films was analyzed using XRD and depicts the amorphous nature of the doped films. All the films are highly transparent, and the value of transparency is around 80 % in the visible region. The optical constants were calculated based on Kramers-Kroning relations. The optical band gap value decreased with doping and is in the range of 2.73 to 2.31 eV. The enhancement in the linear optical properties such as refractive index, absorption index, and dielectric constant was also observed with an increase in the doping concentration. The linear refractive index value increased with doping concentration, and it was in the range of 2.16 to 2.62 indicates that the present sample is useful optical window applications. The nonlinear optical properties such as $\chi^{(1)}$, $\chi^{(3)}$, and $n^{(2)}$ are varying in the range of 0.005 to 0.468, 3.283 × 10^{-142} to 7.746 × 10^{-12} esu, and 7.986 × 10^{-13} to 1.119 × 10^{-10} esu, respectively. The enhancement in the optical properties with increasing doping concentration suggests the present films are useful for various optical device applications. The maximum dielectric constants are varying from 4.54 to 6.42, which indicates that the present samples are suitable for optoelectronic devices. Furthermore, nonlinear optical properties were analyzed and reported.

1. Introduction

The transparent conducting oxide (TCO) based thin films have been attracting many researchers due to its wide variety of applications in the field of display devices, photovoltaic, deicers [1–7]. Thin films of pure and meta doped zinc oxide, tin oxide, indium oxide, and cadmium oxide are extensively used and receive much attention due to its high optical transmittance and conductivity [8–10]. Amongst all the oxides, cadmium oxide (CdO) is an especially exciting material with high carrier mobility, which is the fascinating property to be used in optoelectronic devices [11,12]. It also draws the considerable attention of the researchers due to large conductivity and optical transparency, which are the key to be used in the solar cell [13,14]. However, CdO is exhibit useful properties in pure form due to the defects of oxygen vacancies and cadmium interstitials, and it shows a high resistivity. From the literature, it is learned that the resistivity is decreased by doping the CdO matrix with metal-ions like F-, Mn-, Dy-, and Sn- [15–19].

Among different metal dopants. Indium (In-) is chosen as the dopant in the present paper as it has a similar radius for Cd-ions [20]. Zhu et al. have presented a report on the In: CdO and discussed in the enhancement of electrical properties and an increase in the optical band gap due to the Burstein-Moss effect [21]. There are different growth techniques available to prepare pure and In: CdO films [22–25]. Therefore, it is worthwhile to study the effects of doping on the structural, morphological, optical, and electric properties of CdO.

* Corresponding author at: Department of Physics, Faculty of Science, King Khalid University, P.O. Box 9004, Abha, Saudi Arabia.
E-mail address: ihussein@kku.edu.sa (I.S. Yahia).

https://doi.org/10.1016/j.jnoncrysol.2020.120454
Received 12 May 2020; Received in revised form 11 September 2020; Accepted 22 September 2020

Moreover, for the optical parameter's calculations, a smaller number of reports are available in the literature concerning the use of Kramers-Kronig relations of the optical analysis [27]. Kramers-Kronig dispersion relations are the most useful method for the accurate estimation of the optical parameters. This type of approach is not found in many reports; hence, it makes the present paper more informative.

To the best of our knowledge, there are no reports available on the detailed calculations of linear and nonlinear optical parameters using Kramer's Kronig relations until now for Indium-doped CdO nanostructured films. Thus, it is worthwhile to investigate the linear and nonlinear optical properties of In-doped CdO films using Kramer's Kronig relations.

2. Experimental details

2.1. Preparation method

The undoped and doped samples of In-doped CdO films were coated on highly cleaned glass substrates by a sol-gel spin coating technique. Cadmium acetate, indium chloride, 2-methoxy ethanol, and monoethanolamine were used as starting material, solvent, and stabilizer, respectively. Appropriate amounts of cadmium acetate were dissolved in 2-methoxy ethanol for one hour, and the stabilizer monoethanolamine (MEA) is added to the final solution after another one hour with continuous stirring. The solution was stirred at 60 °C/700 rpm for two hours to obtain a homogeneous solution. The same procedure is repeated for 1, 5, 10, and 15%. The dopant material is taken according to the percentage and converted to a weight added to the pure solution. To get the quality and impurity in fewer values in the as-deposited thin films, glass substrates were cleaned stepwise ultrasonically in soap water, distilled water, and finally in ethanol, respectively. Nitrogen flow was used to remove any alcohol droplets and to have a highly dried and cleaned surface. After preparing solutions, the films were coated on glass substrates with 1500 rpm for 60 sec using the spin coating machine, and the same experimental conditions are repeated to coat successive tenth layers of pure and In-doped CdO samples. The temperature between the successful layers was 120 °C for 10 minutes. The final deposited samples are subjected to the annealing process at 450 °C in a muffle furnace for two hours. The first annealing at 120 °C for the as-prepared films was done after deposition of the film to evaporate the organic solvents and coat successive tenth layers. The second annealing process was done at 450 °C to convert the multi-tenth layers of hydroxide forms of the layers to the oxide form. The final annealed stage is important to remove the residuals of the organic solvent and to stack the layers to form In-doped CdO nanostructured films. Thus, the films were deposited, and thickness was measured by the Alpha-Step IQ surface profile system in KKU. The thickness values of pure and In-doped (1, 5, 10, and 15%) CdO are 150, 153, 148, 159, 149 nm, respectively.

2.2. Measurements & devices

The XRD studies of pure and In-doped CdO thin films were investigated using an X-ray diffractometer (Shimadzu LabX, 6000) with CuK_{α} source of wavelength =1.5406 Å) operated at 30 kV and 30 mA.

The surface morphologies of pure and In-doped CdO films were studied by the Atomic force microscope (AFM) (Solver Next, Russia).

Transmittance, reflectance, absorbance, and other optical parameters were measured and calculated based on the data obtained by JASCO UV-VIS-NIR 570 spectrophotometer in the wavelength range 300-900 nm (UV-Visible region).

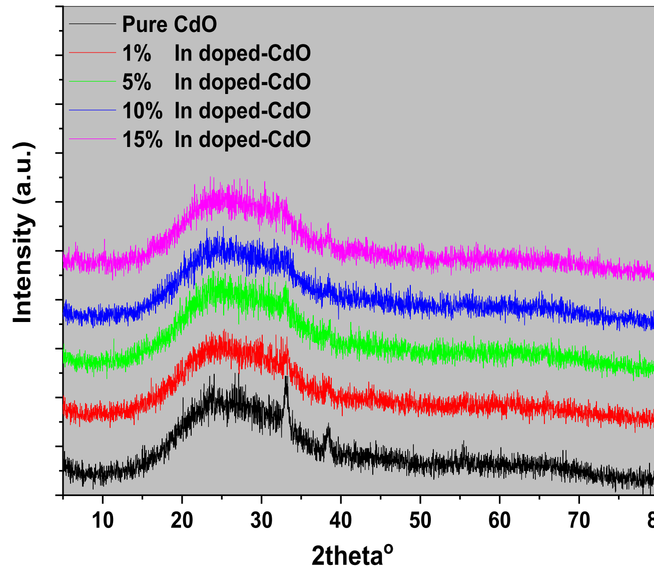

Fig. 1. XRD of In-CdO films deposited with different concentration of In- (0%, 1%, 5%, 10%, and 15%).

3. Results and discussions

3.1. XRD analysis of the pure and In-doped CdO nanostructured films

Fig. 1. showed the XRD patterns of the present samples recorded between 20° and 80°. From the figure, the present films are indicating amorphous. However, for pure CdO, the peaks are observed at 33° and 38°, which tend to disappear by increasing the concentration of Indium-ions in the matrix. The observed peaks are well-matched with JCPDS-Card No. 05-0640 [26]. The reason for the decreasing nature of the peaks with increasing the doping concentration is attributed to the reducing crystallite size, and some deposition conditions were also in correlation with the data available in the literature [27]. The peaks concerning the presence of In_2O_3 are absent confirms that there are no secondary phases formed in the studied film.

3.2. AFM studies of the pure and In-doped CdO nanostructured films

It is well established that the films' optical and electrical properties contribute to the size of the grain. Hence, it is worthwhile to look at the morphology of the pure and In: CdO films. Fig. 2(a,b) shows the surface morphology of pure and In-doped (0, 1, 5, 10, and 15%) CdO films. It is found from these figures that indium changes the grain size and surface roughness of the films with a decrease in grain size with increasing the doping concentration. This decreasing trend for the In-doping is attributed to the grain. Ions occupy the sites of cadmium results in internal stress, thereby decreasing the grain size. A similar trend of increase in grain size up to certain doping levels and decreasing behavior was observed for Y: CdO prepared by spray pyrolysis technique [14,15]. In the present case, the grain size and roughness values are varying from 316 - 95 nm to 79.57 - 38.231 nm, respectively.

3.3. Linear and nonlinear optical properties of the pure and In-doped CdO nanostructured films

For the analysis of the optical properties, the variance of transmittance, reflection, and absorption as a function of wavelength must be considered in our account. Thus, these optical parameters in the wavelength range of 300-900 nm are plotted as a function of the wavelength. Fig. 3(a) showed the transmittance graph of pure and doped samples. All the films in the visible region showed a high transmittance, and the transmittance is about 80 %, and then it decreases with

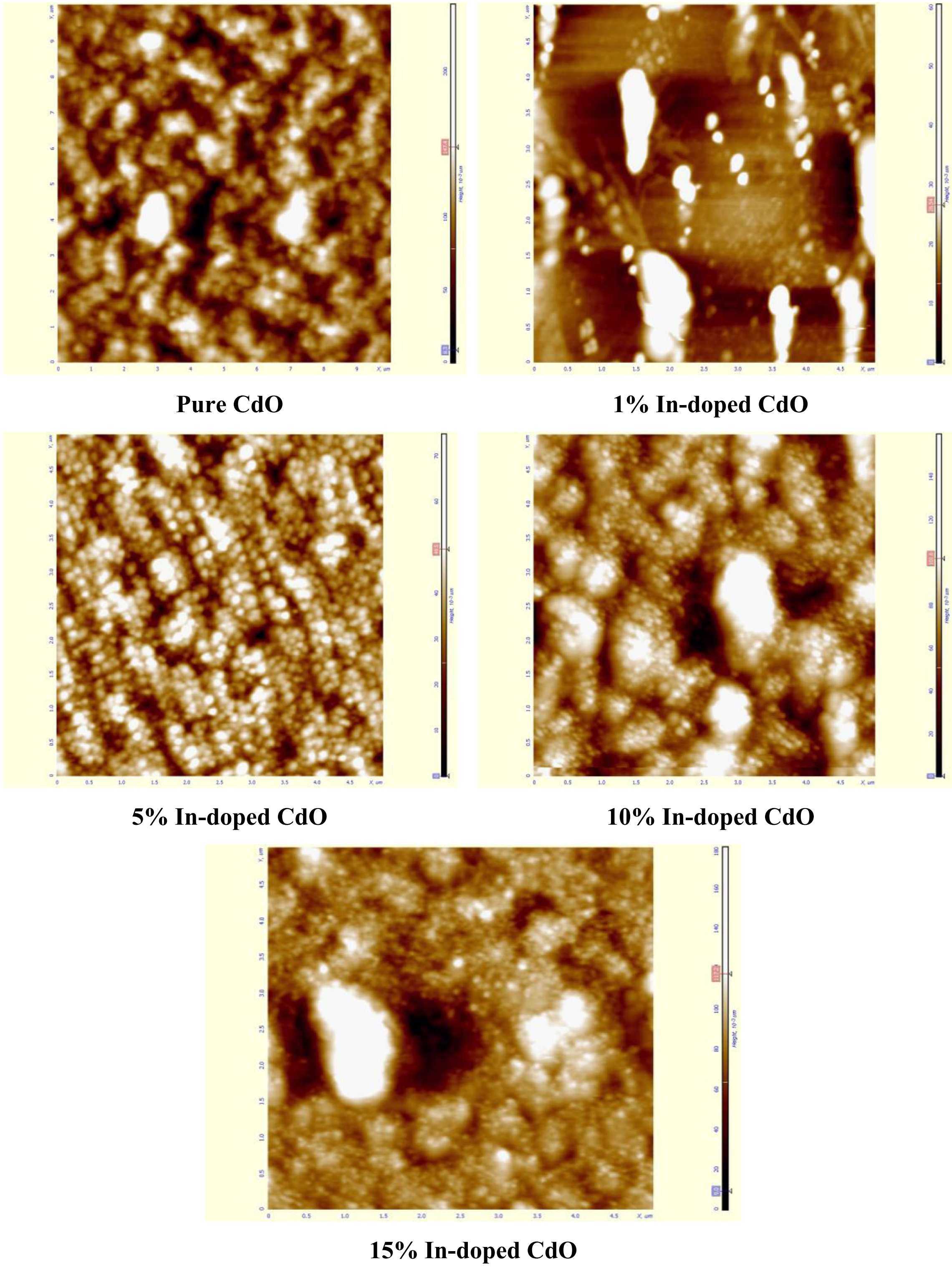

Fig. 2. 2D/AFM images of In-CdO films deposited with different concentration of In- (0%, 1%, 5%, 10%, and 15%).

increasing the doping concentration. The films which are highly transparent in the visible region are studied to enable solar cell applications. Zheng Biju et al. has deposited the In-doped CdO prepared by pulse laser deposition method, and the transmittance is observed in the range of 75 % - 85 % [28]. The decrease in the transmittance may be attributed to the In-ions occupying the interstitial positions and tending to increase the absorption. A similar trend is observed in present samples suggested that the same phenomenon of Zheng Bijuet.al is applicable for our samples [28].

Fig. 3(b) shows the absorption spectra in the wavelength range of 300-900 nm, and it is found that the absorbance edge increase with doping concentration. It showed a bump in the UV-region and flattens in the visible area, which making these films to have application in many optoelectronic devices. Similar behavior is observed in many oxide films like CdO, NiO, etc. and presented in several reports [28,29].

The reflectance is an essential property for an optoelectronic device. The reflectance is plotted as a function of wavelength in the range of 300-900 nm (see Fig. 3c). From these plots, it is observed that the

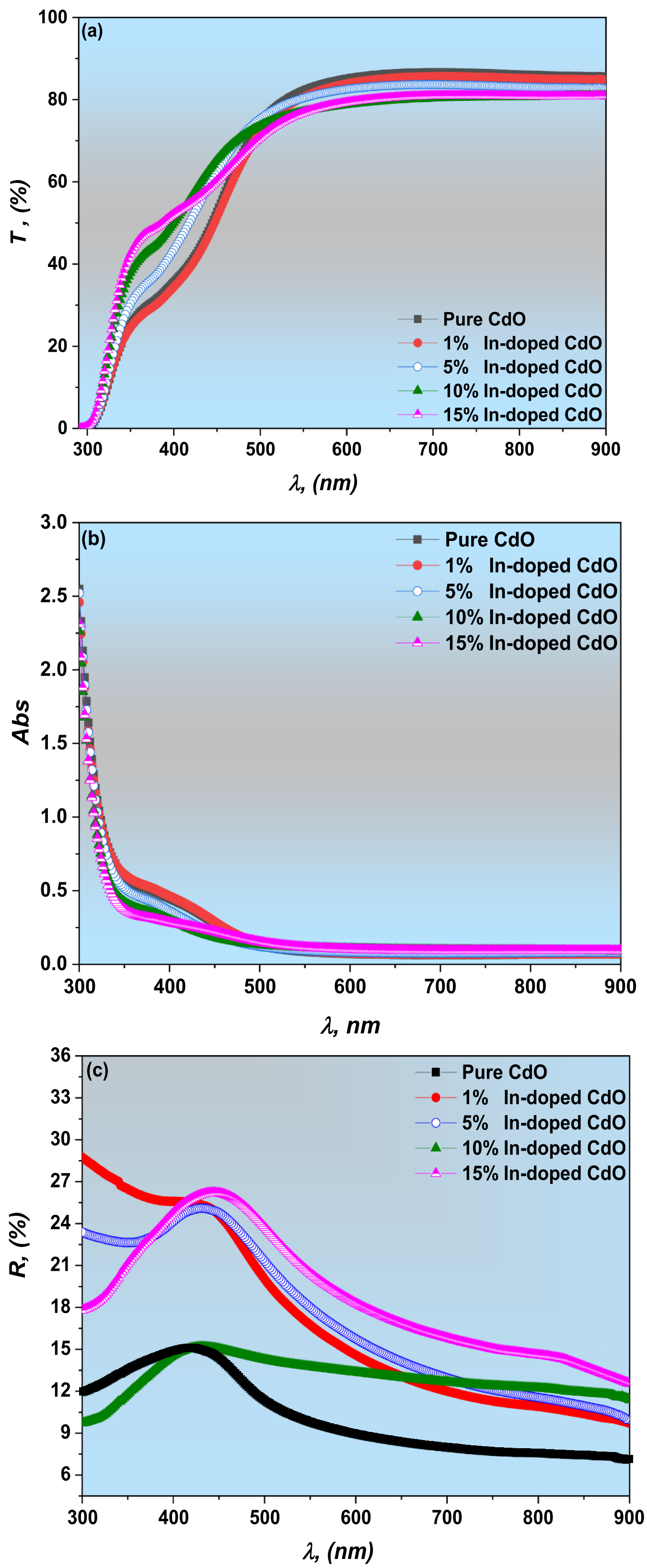

Fig. 3. (a-c): Transmittance, Absorbance, Reflectance of In-CdO films deposited with different concentration of In- (0%, 1%, 5%, 10%, and 15%).

reflectance increases with an increase in the concentration of In-doping into CdO. Furthermore, the transmittance observed in this case is very high compared to the previously recorded data on various growth techniques, indicating that the current samples have more optical/optoelectronic applications [28].

3.3.1. Kramers-Kronig relations for determining both the refractive index and the extinction coefficient

Due to the importance of optical applications and optical electronics, the optical constants are fundamental to determine by an accurate method. All calculated methods of optical constant based on the thin film thickness, and it is considered a significant issue since there is no particular device to measure the thickness. The Kramer-Kronig approach is the best solution for the accurately optical constant calculations without relying on the film thickness [29–36]. The optical constants, including the refractive index *n* and the extinction coefficient *k*, can be calculated for CdO thin films were calculated from the Kramers-Kronig approach as [29–36]:

$$N'(\omega) = n(\omega) + ik(\omega), \tag{1}$$

$$n(\omega) = \frac{1 - R(\omega)}{1 + R(\omega) - 2\sqrt{R(\omega)}cos\phi(\omega)}, \tag{2}$$

$$k(\omega) = \frac{2\sqrt{R(\omega)}sin\phi(\omega)}{1 + R(\omega) - 2\sqrt{R(\omega)}cos\phi(\omega)}, \tag{3}$$

where ω is the angular frequency, and the $\phi(\omega)$ is the phase difference among the incident and the reflected radiations and was derived from the Fourier transform of *K-K* dispersion relation as [29–36]:

$$\varphi(\omega) = -\left(\frac{\omega}{\pi}\right)\int_0^\infty \frac{lnR(\omega') - lnR(\omega)}{\omega'^2 - \omega^2}d\omega', \tag{4}$$

The Fourier transform of Eq. (3) is as follow [29–36]:

$$\varphi(\omega_i) = \frac{4\omega_i}{\pi} \times \Delta\omega_i \times \sum_i \frac{ln\sqrt{R(\omega)}}{\omega_i'^2 - \omega_j'^2}, \tag{5}$$

where

$$\Delta\omega_j = \omega_{j+1} - \omega_j, \tag{6}$$

where i =2, 4, 6,..., j-1, j+1,... for odd j and i =1, 3, 5,..., j-1, j+1,... for even j. Thus, in Fig. 4(a,b), the calculated refractive index and the extinction coefficient is plotted as a function of wavelength, respectively. The refractive index showed a normal dispersion (i.e., decreases with increasing the wavelength) and anomalous dispersion (i.e., increases with increasing the wavelength) for the studied nano-materials. The maximum refractive index and their related wavelength for the studied materials are represented inTable 2. The maximum refractive index increased with increasing the In-doping ratio in the CdO matrix. Also, the extinction coefficient showed a maximum value in the studied wavelength region, as shown in Fig. 4b, and Table 2. The maximum extinction coefficient increased with increasing the In-doping ratio in the CdO matrix (see Table 2). Both *n* and *k* increase as the doping of In-ions into the CdO matrix increases. This may be attributed to the improvement of the polarizability and the film density. The lower values of *k* suggested that the films are transparent, which is seen from the transmission data of the studied films.

3.3.2. Linear optical properties

The bandgap, which is necessary for many optical applications, is evaluated from the following relation:

$$(\alpha E)^h = Q(E - E_g) \tag{7}$$

where ($\boldsymbol{\alpha} = 4\pi k/\lambda$) is the absorption coefficient given by edge in the band to band transition [37]. Here, Q is a constant; E is the energy of photons, E_g is the energy bandgap, and h is a constant. This h determines the electronic transition type, 2 for direct transition, and 1/2 for the indirect transition. The direct bandgap as a function of photon energy is plotted in Fig. 5. The bandgap is found to decline from the figure, with an increase in the doping concentration. From this figure,

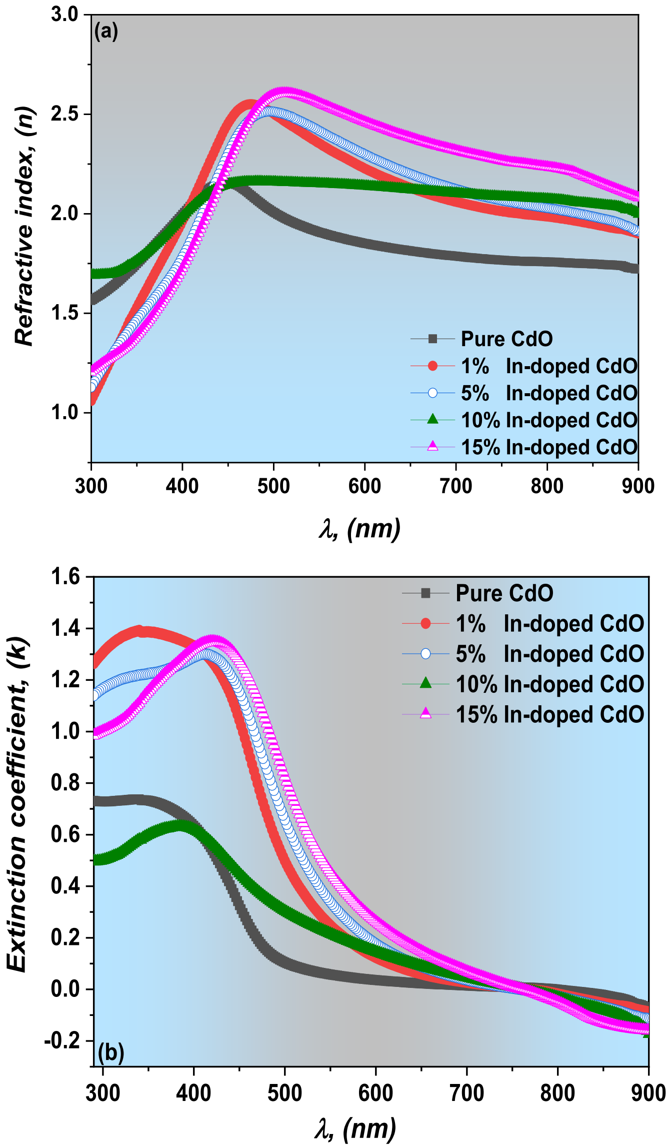

Fig. 4. (a,b): Refractive index and extinction coefficient as a fucntion of wavlenght of In-CdO films deposited with different concentration of In- (0%, 1%, 5%, 10%, and 15%).

Table 1
The AFM parameters of In-doped CdO nanostructured thin films.

Samples	Grain size, (nm)	Roughness, (nm)
Pure CdO	316	79.5
1 % In-doped CdO	133	42.6
5% In-doped CdO	163	48.6
10% In-doped CdO	113	36.5
15% In-doped CdO	95	38.2

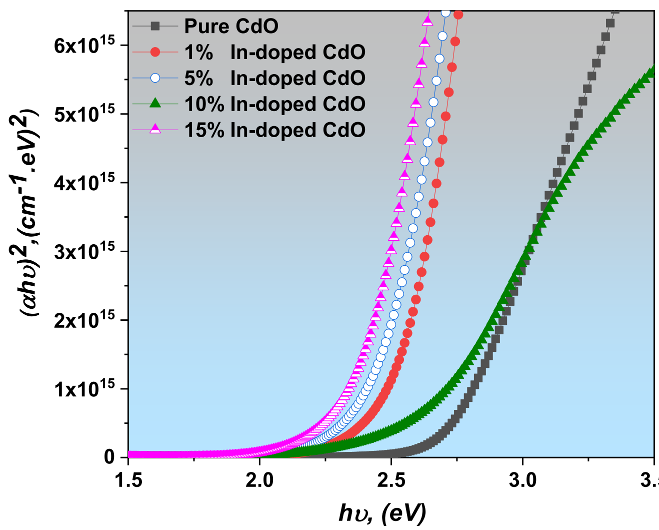

Fig. 5. Energy band gap analysis of In-CdO films deposited with different concentration of In- (0%, 1%, 5%, 10%, and 15%).

Table 3
The optical band gap for undoped CdO and 1%, 5%, 10%, 15% In-doped CdO compared with other work.

Samples	Bandgap values, (eV)	References
Pure CdO	2.73	Present work
1 % In-doped CdO	2.61	
5% In-doped CdO	2.44	
10% In-doped CdO	2.36	
15% In-doped CdO	2.31	
Ce-doped CdO	2.1 – 4.2 eV	[48]
Al doped CdO	2.32 - 2.54 eV	[49]
N doped CdO	3.92 - 3.98 eV	[50]

the bandgap is observed to decrease with increasing the doping concentration. Besides, the bandgap values are in the range from 2.73 eV to 2.31 eV, which is consistent with the data recorded in the literature for CdO films [28]. The decrease in the transmittance of the films results in the reduction of energy gap values and attributed to the variation of the thickness of the films with doping. The observed bandgap values are quite high from previously reported of Kramers–Kronig approach, and these make them useful for optoelectronic device applications. The comparative study of band gap values is tabulated in Table 3.

The optical dielectric constant ε is the key property of the material, which gives information about the retardation of light and energy absorption. The complex dielectric constant is given by $\varepsilon^* = \varepsilon_r + i\varepsilon_i$. From the values of k and n, both ε_r (dielectric constant) and ε_i (dielectric loss) can be calculated from the following equations [38]:

$$\varepsilon_r = n^2 - k^2 \quad (8)$$

$$\varepsilon_i = 2nk \quad (9)$$

The lower value of the dielectric loss makes the tested samples available for optoelectronic devices. Fig. 6(a,b) showed the variation of dielectric constant and dielectric loss of the present films. From this

Table 2
The maximum values of the refractive index and the extinction coefficient of the prepared In-doped CdO nanostructured thin films.

Samples	Refractive index		Extinction coefficient	
	Wavelength, (nm)	Maxium (n)	Wavelength, (nm)	Maximum (k)
Pure CdO	442	2.171	359	0.727
1% In-doped CdO	475	2.564	340	1.407
5% In-doped CdO	490	2.526	414	1.293
10% In-doped CdO	464	2.166	388	0.639
15% In-doped CdO	509	2.612	423	1.362

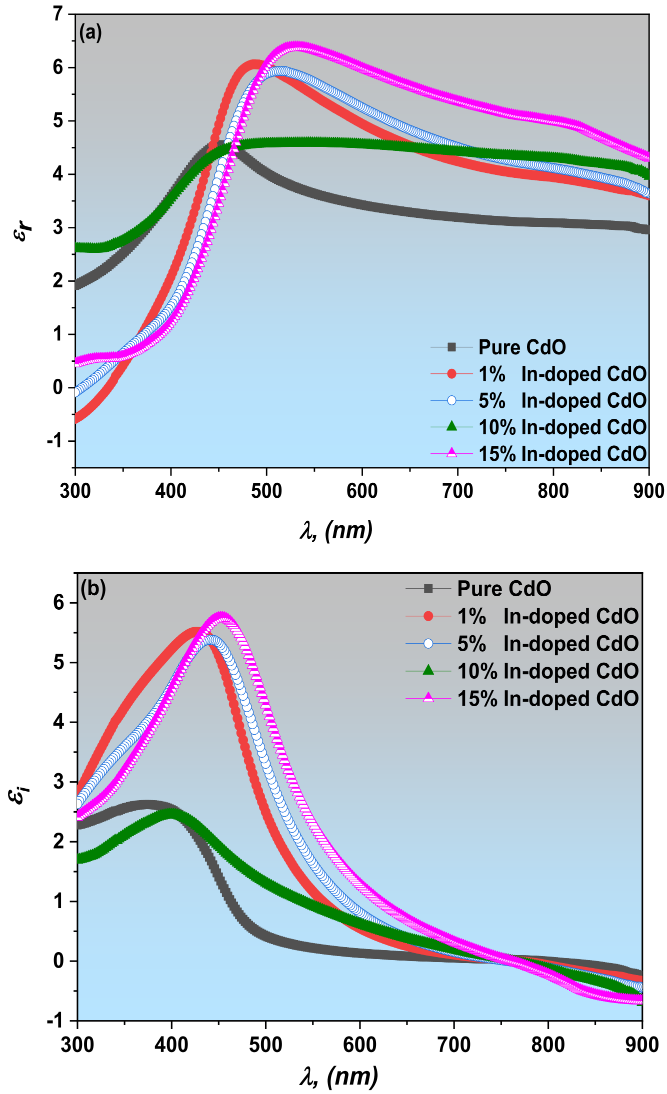

Fig. 6. (a,b): Both ε_r (dieletric constant) and ε_i (dieletric loss) as a fucntion of wavlenght of In-CdO films deposited with different concentration of In- (0%, 1%, 5%, 10%, and 15%).

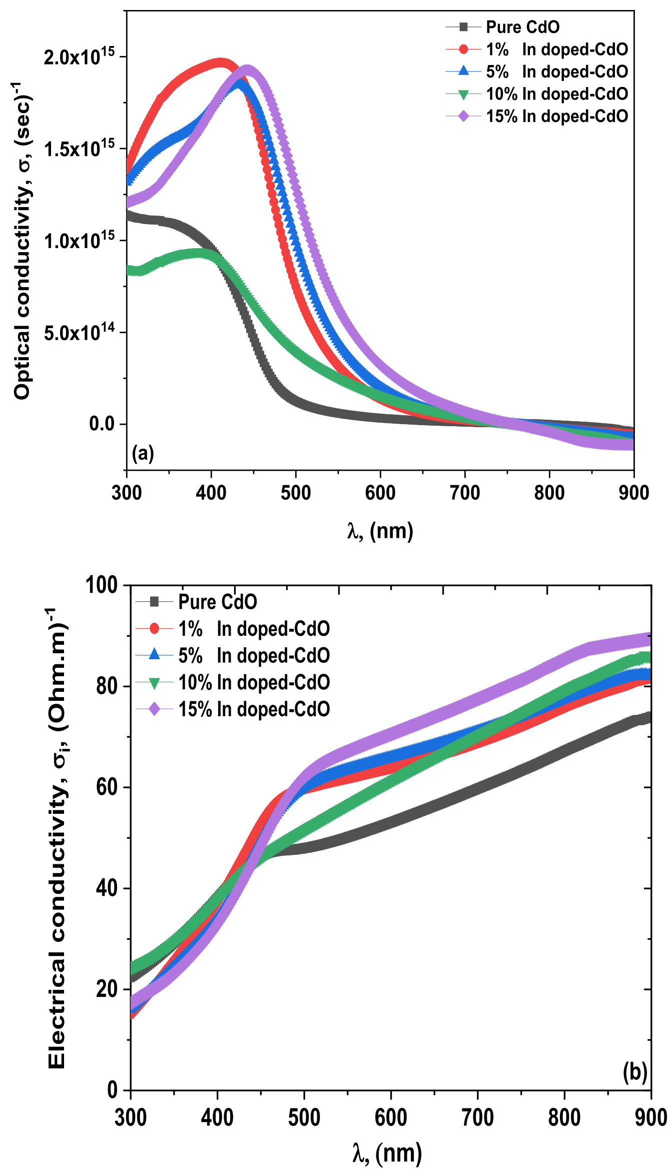

Fig. 7. (a,b): Optical conductivity (σ) and electrical condcuivity (σ_i) as a fucntion of wavlenght of In-CdO films deposited with different concentration of In- (0%, 1%, 5%, 10%, and 15%).

figure, with doping concentration, the dielectric constant increases, and the dielectric loss decreases. The observed values are comparable and high, with earlier studies indicating that the samples present are useful in many optical devices. Beside it is found that the values of the dielectric constant are in the range -0.573 – 6.424 while, the values of the dielectric loss are in the range -0.662 – 5.781.

The optical conductivity of the studied thin films gives accurate information about the absorption processes, where their applications are located. Optical conductivity is calculated from the following equation. [39]

$$\sigma = \frac{\alpha n c}{4\pi} \tag{10}$$

where α being the absorption coefficient, n being the refractive index, and c is the speed of light ($3 \times 10^8\, m$/sec). Fig. 7(a) indicates the optical conductivity of pure and In-doped CdO films. The increase in optical conductivity was found in In: CdO film with increase doping concentration. For all samples, it is found that σ is in the range -1.094×10^{14} – 1.978×10^{11}. The electrical conductivity (σ_e) of In: CdO thin films is determined by the formula [40].

$$\sigma_e = \frac{2\lambda\sigma_{op}}{\alpha}, \tag{11}$$

where λ is the wavelength, is shown in Fig. 7(b) From this figure, it is clear that (σ_e) decreases with photon energy, and it is the range 14.751 – 89.557 for all the samples. From Fig. 7b, the electrical conductivity values are showing considerable variation. This suggested that In-ions increases the charge carriers with doping percentage, and these samples are useful for electro-optic applications. Both the optical and electrical conductivities are comparable to other metal oxide thin films [41].

3.3.3. Nonlinear optical properties

The effect of light on the metal oxide thin films is essential for optical device applications. When the high-intensity light, like a laser, is allowed to fall on the film surface, a non-linear behavior is observed. For normal light intensity, the induced polarization (P) is directly proportional to the electrical field (E). The induced polarization (P) is a non-linear property of an electrical field (E), for laser-like light. Therefore, the nonlinear refractive index (n_2) and third-order nonlinear optical susceptibilities ($\chi^{(3)}$) of the pure and In- doped CdO thin films need to be examined. In terms of nonlinear polarizability (PNL), the polarizability (p) is given by [42]:

$$p = \chi^{(1)}E + P_{NL} \quad (12)$$

where $P_{NL} = \chi^{(2)}E^2 + \chi^{(3)}E^3$and $\chi^{(1)}, \chi^{(2)}$ and $\chi^{(3)}$ are the linear, second, and third-order nonlinear optical susceptibilities, respectively. The direct refractive index $n\ (\lambda)$ can be calculated as follows [43,44]:

$$n(\lambda) = n_o(\lambda) + n_2(E^2) \quad (13)$$

The parameter $n\ (\lambda)$ is defined as: $n_o\ (\lambda) >> n_2(\lambda)$, $n(\lambda)\ =\ n_o(\lambda)$ and (E^2) is mean square values of electric field. $\chi^{(1)}$ can be known from the following equation [43,44]:

$$\chi^{(1)} = \frac{{n_0}^2 - 1}{4\pi}, \quad (14)$$

The third-order nonlinear optical susceptibility $(\chi^{(3)})$ follows the relation [45–47]:

$$\chi^{(3)} = A\ (\chi^{(1)})^4, \quad (15)$$

From Eqs. (9) and (10), we get the following equation:

$$\chi^{(3)} = A\left(\frac{{n_o}^2 - 1}{4\pi}\right)^4, \quad (16)$$

where A is given by 1.7×10^{-10} esu [45]. Thus, n_2 can be obtained from the equation [45,46]:

$$n_2 = \frac{12\pi\chi^{(3)}}{n_0} \quad (17)$$

For the pure and In-doped CdO films, the variance of linear, third-order nonlinear optical susceptibilities and nonlinear refractive index as a function of wavelength is studied and shown in Fig. 8(a-c). With wavelength, these values are increased and reach a maximum value in the visible region and achieve a constant value at the higher wavelengths. Moreover, these values tend to increase with the increase the doping concentration. The nonlinear refractive index is derived from third-order nonlinear optical susceptibility; it shows a similar fashion and is displayed in Fig. 8c. The values of $\chi^{(1)}$ and $\chi^{(3)}$ are from 0.005 to 0.468, and 3.283×10^{-142} to 7.746×10^{-12} esu, respectively. The value of the nonlinear refractive index (n_2) is varying between 7.986×10^{-13} to 1.119×10^{-10} esu, and all the optical parameters were tabulated in Table 3. From this table, it is clearly understood that the present Indium as a dopant showed a considerable impact on the host CdO materials and would have a significant effect on the application of photonic devices [48].

4. Conclusion

Pure and In-doped CdO films were successfully produced using a sol-gel assisted spin coating technique. The films of fine quality were obtained, and the structural, morphological properties were analyzed. The optical bandgap for pure and In-doped CdO samples was found to be in the range of 2.73 to 2.31 eV, and bandgap decrease was observed as a result of doping. The dielectric constant and optical conductivity were found to be varying with increasing the doping concentration. The nonlinear optical properties were studied extensively, and the values of linear optical susceptibility, third-order nonlinear optical susceptibility, and nonlinear refractive index 0.005 to 0.468, 3.283×10^{-142} to 7.746×10^{-12} esu, and 7.986×10^{-13} to 1.119×10^{-10} esu, respectively are reported. From all the linear and nonlinear optical properties, the present In-doped CdO is showing a considerable impact on the host CdO material, which suggests that the fabricated films are suitable for optoelectronic devices and solar cells applications.

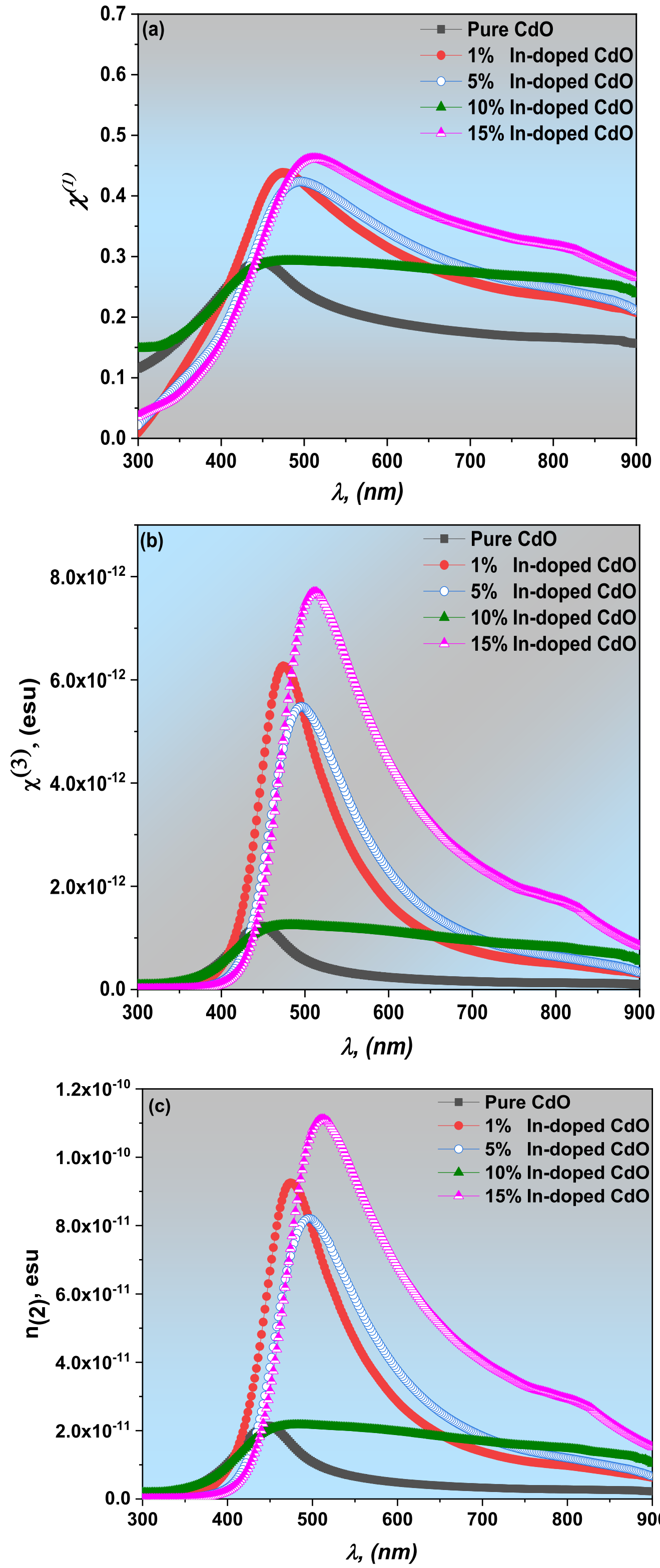

Fig. 8. (a-c): $\chi^{(1)}$, $\chi^{(3)}$ and n_2 as a fucntion of wavlenght In-CdO films deposited with different concentration of In- (0%, 1%, 5%, 10%, and 15%).

Authors' contribution

V. Ganesh: Conceptualization, Methodology, Data curation, Writing- Original draft preparation and editing

L.Haritha: Validation, Software, Writing- Original draft preparation, reviewing and editing

H. Elhosiny Ali: Investigation, Writing- Original draft preparation

A.M. Aboraia: Calculation and solving of Kramers-Kronig relations

Yasmin Khairy: Validation, Software

H.H. Hegazy:: Calculation and solving of Kramers-Kronig relations

V. Butova: Visualization, Writing- Original draft preparation

Alexander V.Soldatov: Investigation, Writing- Original draft preparation
H. Algarni: Supervision, Conceptualization
H.Y. Zahran: Validation, Software
I.S. Yahia: Supervision, Conceptualization

Declaration of Competing Interest

Declaration of Conflict of Interest On behalf of all authors, we, the corresponding authors hereby confirm that the manuscript submitted under the title "**The detail calculation of optical properties of Indium-doped CdO nanostructured films using Kramers-Kronig relations**" has no conflict of interest. The authors have no involvement in any organization or entity with any financial interest or non-financial in the subject matter or materials discussed in this manuscript. We further declare that this manuscript is original, has neither been published nor currently being considered for publication elsewhere.

Acknowledgment

The authors extend their appreciation to the Deanship of Scientific Research at King Khalid University for funding this work through research groups program under grant number R.G.P. 2/50/40

References

[1] A.V. Moholkara, G.L. Agawanec, K.-U. Sima, Y.-B. Kwona, K.Y. Rajpurec, J.H. Kim, Influence of deposition temperature on morphological, optical, electrical and opto-electrical properties of highly textured nano-crystalline spray deposited CdO: Ga thin films, Appl. Surf. Sci. 257 (2010) 93–101 https://doi.org/10.1016/j.apsusc.2010.06.043.
[2] F.F. Yang, L. Fang, S.F. Zhang, J.S. Sun, Structure and electricalproperties of $CdIn_2O_4$ thin films prepared by DC reactive magnetron sputtering, Appl. Surf. Sci. 254 (2008) 5481–5486 https://doi.org/10.1016/j.apsusc.2008.02.090.
[3] G. Murtaza, B. Amin, S. Arif, M. Maqbool, Structural, electronic and optical properties of $CaxCd_{1-x}O$ and its conversion from semimetal to wide bandgap semiconductor, Comput. Mater. Sci. 58 (2012) 71–76 https://doi.org/10.1016/j.commatsci.2012.01.020.
[4] S. Salam, M. Islam, A. Akram, Sol–gel synthesis of intrinsic and aluminum-doped zinc oxide thin films as transparent conducting oxides for thin film solar cells, Thin Solid Films 529 (2013) 242–247 https://doi.org/10.1016/j.tsf.2012.10.079.
[5] H. Hosono, H. Ohta, M. Orita, K. Ueda, M. Hirano, Frontier of transparent conductive oxide thin films, Vacuum 66 (2002) 419–425 https://doi.org/10.1016/S0042-207X(02)00165-3.
[6] D.S. Ginley, C. Bright, Transparent conducting oxides, MRS Bull. 25 (2000) 15–18 https://doi.org/10.1557/mrs2000.256.
[7] T.J. Coutts, D.L. Young, X. Li, W.P. Mulligan, X. Wu, Search for improved transparent conducting oxides: a fundamental investigation of CdO, $Cd_2 SnO_4$, and $Zn_2 SnO_4$, J. Vac. Sci. Technol. A 18 (2000) 2646–2660 https://doi.org/10.1116/1.1290371.
[8] Y Kim S, K Hong, L Lee J, et al., Enhancement of physical properties of indium tin oxide deposited by super density arc plasma ion plating by O_2 plasma treatment, Solid-State Electron 52 (2008) 1–6 https://doi.org/10.1016/j.sse.2007.07.037.
[9] Z Yang, Y Huang, G Chen, et al., Ethanol gas sensor based on Al-doped ZnO nanomaterial with many gas diffusing channels, Sens. Actuat. B 140 (2009) 549–556 https://doi.org/10.1016/j.snb.2009.04.052.
[10] S. Aksoy, S.Ilican Y.Caglar, M. caglar, Effect of heat treatment on physical properties of CdO films deposited by sol–gel method, Int. J. Hydrogen Energy 34 (2009) 5191–5195 https://doi.org/10.1016/j.ijhydene.2008.09.057.
[11] M. Yan, M. Lane, C.R. Kaneewurf, R.P.H. Chang, Highly conductive epitaxial CdO thin films prepared by pulsed laser deposition, Appl. Phys. Lett. 78 (2001) 2342–2344 https://doi.org/10.1063/1.1365410.
[12] B.G. Lewis, D.C. Paine, Applications and processing of transparent conducting oxides, Mater. Res. Soc. Bull. 25 (2000) 22–27 https://doi.org/10.1557/mrs2000.147.
[13] R. Ferro, J.A. Rodriguez, O. Vigil, A. Morales-Acevado, G. Contreras-Puente, CdO thin films deposited by spray pyrolysis, Phys. Stat. Solidi. A 177 (2000) 477–483 https://doi.org/10.1002/(SICI)1521-396X(200002)177:2≤477::AID-PSSA477≥3.0.CO;2-3.
[14] R.S. Mane, H.M. Pathan, C.D. Lokhande, S.H. Han, An effective use of nanocrystalline CdO thin films in dye-sensitized solar cells, Sol. Energy 80 (2006) 185–190 https://doi.org/10.1016/j.solener.2005.08.013.
[15] M. Kul, M. Zor, A.S. Aybek, S. Irmak, E. Turan, Some structural properties of CdO:F films produced by ultrasonic spray pyrolysis method, Thin Solid Films 515 (2007) 8590–8593 https://doi.org/10.1016/j.tsf.2007.03.104.
[16] V. Bilgin, I. Akyuz, S. Kose, F. Atay, Characterization of Mn-incorporated CdO films grown by ultrasonic spray pyrolysis, Semicond. Sci. Technol. 21 (2006) 579–582 https://doi.org/10.1088/0268-1242/21/5/001.
[17] T. Chen, Q.J. Liu, Z.L. Zhou, Y.D. Wang, et al., A high sensitivity gas sensor for formaldehyde based on CdO and In_2O_3 doped nanocrystalline SnO_2, Nanotechnology 19 (2008) 095506https://doi.org/10.1088/0957-4484/19/9/095506.
[18] A. Dakhel A, Influence of dysprosium doping on the electrical and optical properties of CdO thin films, Sol. Energy 83 (2008) 934–939 https://doi.org/10.1016/j.solener.2008.12.015.
[19] Z. Zhao, D.L. Morel, C.S. Ferekides, Electrical and optical properties of tin-doped CdO films deposited by atmospheric metalorganic chemical vapor deposition, Thin Solid Films 413 (2002) 203–211 https://doi.org/10.1016/S0040-6090(02)00344-9.
[20] S. Jin, Y. Yang, J.E. Medvedeva, L. Wang, S. Li, N. Cortes, J.R. Ireland, A.W. Metz, J. Ni, M.C. Hersam, A.J. freeman, Tuning the properties of transparent oxide conductors. Dopant ion size and electronic structure effects on CdO-based transparent conducting oxides Ga-and In-doped CdO thin films grown by MOCVD, Chem. Matter 20 (2007) 220–230 https://doi.org/10.1021/cm702588m.
[21] Y. Zhu, R.J. Mendelsberg, J. Zhu, J. Han, A. Anders, Transparent and conductive indium doped cadmium oxide thin films prepared by pulsed filtered cathodic arc deposition, Appl. Surf. Sci. 265 (2013) 738–744 https://doi.org/10.1016/j.apsusc.2012.11.096.
[22] M. A. Flores, R. Castanedo, G. Torres, O. Zelaya, Optical, electrical and structural properties of indium-doped cadmium oxide films obtained by the sol–gel technique. Sol. Energy Mater. Sol. Cells. 93(2009)28-32. https://doi.org/10.1016/j.solmat.2008.02.006.
[23] S. Vijayalakshmi, S. Venkataraj, R. Jayavel, Characterization of cadmium doped zinc oxide (Cd:ZnO) thin films prepared by spray pyrolysis method, J. Phys. D 41 (2008) 245403https://doi.org/10.1088/0022-3727/41/24/245403.
[24] Z. Zhao, D.L. Morel, C.S. Ferekides, Electrical and optical properties of tin-doped CdO films deposited by atmospheric metalorganic chemical vapor deposition, Thin Solid Films 413 (2002) 203–211 https://doi.org/10.1016/S0040-6090(02)00344-9.
[25] B. Saha, R. Thapa, K.K. Chattopadhyay, Bandgap widening in highly conducting CdO thin film by Ti incorporation through radio frequency magnetron sputtering technique, Solid State Commun. 145 (2008) 33–37 https://doi.org/10.1016/j.ssc.2007.10.001.
[26] B.J. Zheng, J.S. Lian, L. Zhao, Q. Jiang, Optical and electrical properties of In-doped CdO thin films fabricated by pulse laser deposition, Appl. Surf. Sci. 256 (2010) 2910–2914 https://doi.org/10.1016/j.apsusc.2009.11.049.
[27] JCPDS—International Centre for Diffraction Data, Card No. 05-0640, 1997.
[28] Zheng Biju, Hu Wen, Influence of substrate temperature on the structural and properties of In-doped CdO films prepared by PLD, J. Semicond. 34 (2013) 053003https://doi.org/10.1088/1674-4926/34/5/053003.
[29] E. Pakizeh, Optical response and structural properties of Fe-doped Pb $(Zr_{0.52} Ti_{0.48})O_3$ nanopowders, J. Mater. Sci. 31 (2020) 4872–4881 https://doi.org/10.1007/s10854-020-03050-1.
[30] F. Behzadi, E. Saievar-Iranizad, E. Pakizeh, Optical study on single-layer photoluminescent graphene oxide nanosheets through a simple and green hydrothermal method, J. Photochem. Photobiol. A 364 (2018) 595–601 https://doi.org/10.1016/j.jphotochem.2018.06.047.
[31] E. Pakizeh, M. Moradi, Effect of particle size on the optical properties of lead zirconate titanate nanopowders, J. Am. Ceram. Soc. 101 (2018) 5335–5345 https://doi.org/10.1111/jace.15792.
[32] F. Reading, Optical Properties of Solids, first ed., Elsevier; Academic Press, 1972.
[33] A.M. Aboraia, A.A.A. Darwish, V. Polyakov, E. Erofeeva, V. Butova, H.Y. Zahran, A.F. Abd El-Rehim, H. Algarni, I.S. Yahia, A.V. Soldatov, Structural characterization and optical properties of zeolitic imidazolate frameworks (ZIF-8) for solid-state electronics applications, Opt. Mater. 100 (2020) 109648https://doi.org/10.1016/j.optmat.2019.109648.
[34] A.A.A. Darwish, A.M. Aboraia, A.V. Soldatov, I.S. Yahia, Deposition of rhodamine B dye on flexible substrates for flexible organic electronic and optoelectronic: optical spectroscopy by Kramers-Kronig analysis, Opt. Mater.. 95(2019)109219. https://doi.org/10.1016/j.optmat.2019.109219.
[35] M.A. Manthrammel, A.M. Aboraia, M. Shkir, I.S. Yahia, M.A. Assirif, H.Y. Zahran, V. Ganesh, S. AlFaify, A.V. Soldatov, Optical analysis of nanostructured rose bengal thin films using Kramers–Kronig approach: new trend in laser power attenuation, Opt. Laser Technol. 112 (2019) 207–214 https://doi.org/10.1016/j.optlastec.2018.11.024.
[36] M.A. Assiri, M. Aslam Manthrammel, A.M. Aboraia, I.S. Yahia, H.Y. Zahran, V. Ganesh, M. Shkir, S. AlFaify, A.V Soldatov, Kramers–Kronig calculations for linear and nonlinear optics of nanostructured methyl violet (CI-42535): new trend in laser power attenuation using dyes, Physica B 552 (2019) 62–70 https://doi.org/10.1016/j.physb.2018.09.040.
[37] M.M. El-Nahass, K.F. Abd-El-Rahman, A.A.M. Farag, A.A.A. Darwish, Optical characterization of thermally evaporated nickel phthalocyanine thin films, Int. J. Mod. Phys.. 18(2004)421-434. https://doi.org/10.1142/S0217979204023982.
[38] M. Sesha Reddy, K.T. Ramakrishna Reddy, B.S. Naidu, P.J. Reddy, Optical constants of polycrystalline $CuGaTe_2$ films, Opt. Mater. 4 (1995) 787–790 https://doi.org/10.1016/0925-3467(95)00039-9.
[39] F. Bourguiba, A. Dhahri, T. Tahri, K. Taibi, J. Dhahri, E.K. Hlil, Structural, optical spectroscopy, optical conductivity and dielectric properties of $BaTi_{0.5}(Fe_{0.33}W_{0.17})O_3$ perovskite ceramic, B Mater. Sci. 39 (2016) 1765–1774, https://doi.org/10.1007/s12034-016-1305-9.
[40] H.S. Bolarinwa, M.U. Onuu, A.Y. Fasasi, S.O. Alayande, L.O. Animasahun, I.O. Abdulsalami, O.G. Fadodun, I.A. Egunjobi, Determination of optical parameters of zinc oxide nanofibre deposited by electrospinning technique, J. Taibah Univ. Sci.

11 (2017) 1245–1258 https://doi.org/10.1016/j.jtusci.2017.01.004.
[41] Shkir Mohd, V. Ganesh, S. AlFaify, I.S. Yahia, H.Y. Zahran, Tailoring the linear and nonlinear optical properties of NiO thin films through Cr^{3+} doping, J. Mater. Sci. Mater. Electron. (2018), https://doi.org/10.1007/s10854-018-8626-y.
[42] M. Frumar, J. Jedelský, B. Frumarova, T. Wagner, M. Hrdlička, Optically and thermally induced changes of structure, linear and non-linear optical properties of chalcogenides thin films, J. Non-Cryst. Solids 326 (2003) 399–404 https://doi.org/10.1016/S0022-3093(03)00446-0.
[43] H. Ticha, L. Tichy, Semiempirical relation between non-linear susceptibility (refractive index), linear refractive index and optical gap and its application to amorphous chalcogenides, J. Optoelectron. Adv Mater. 4 (2002) 381–386.
[44] V. Ganesh, I. Yahia, S. AlFaify, M. Shkir, Sn-doped ZnO nanocrystalline thin films with enhanced linear and nonlinear optical properties for optoelectronic applications, J. Phys. Chem. Solids 100 (2017) 115–125 https://doi.org/10.1016/j.jpcs.2016.09.022.
[45] C.C. Wang, Empirical relation between the linear and the third-order nonlinear optical susceptibilities, Phys. Rev. B 2 (1970) 2045 https://doi.org/10.1103/PhysRevB.2.2045.
[46] J. Wynne, Nonlinear optical spectroscopy of $\chi^{(3)}$ in $LiNbO_3$, Phys. Rev. Lett. 29 (1972) 650 https://doi.org/10.1103/PhysRevLett.29.650.
[47] D. Hanna, Handbook of Laser Science and Technology, Taylor & Francis, 1988.
[48] V. Ganesh, L. Haritha, H. Elhosiny Al, A.M. Aboraia, Y. Khairy, H.H. Hegazy, V. Butova, A.V. Soldatov, H. Algarni, H.Y. Zahran, I.S. Yahia, Detailed investigation of optical linearity and nonlinearity of nanostructured Ce-doped CdO thin films using Kramers–Kronig relations, Appl. Phys. A 126 (2020) 551 https://doi.org/10.1007/s00339-020-03727-8.
[49] I.S. Yahia, G.F. Salem, M.S. Abd El-sadek, F. Yakuphanoglu, Optical properties of Al-CdO nano-clusters thin films, Superlattices Microstruct. 64 (2013) 178–184 https://doi.org/10.1016/j.spmi.2013.09.024.
[50] V. Ganesh, Mohd Shkir, S. AlFaify, I.S. Yahia, H.Y. Zahran, A.F. Abd El-Rehim, Study on structural, linear and nonlinear optical properties of spin coated N doped CdO thin films for optoelectronic applications, J. Mol. Struct. 1150 (2017) 523–530 https://doi.org/10.1016/j.molstruc.2017.08.047.